Journal of Computational and Applied Mechanics, Vol. 19, No. 1, (2024), pp. 17–35
DOI: 10.32973/jcam.2024.002

NUMERICAL STUDY OF ICE ACCRETION ON BLADE SURFACE WITH VARYING CLOUD CHARACTERISTICS

Ibrahim Kipngeno Rotich
Doctoral School of Environmental Sciences
Eötvös Loránd University, Budapest
ibrahimrkipp@gmail.com

László E. Kollár
Savaria Institute of Technology
Eötvös Loránd University, Budapest
kl@inf.elte.hu

[Received: January 28, 2024; Accepted: April 15, 2024]

Abstract. Wind turbines experience the threat of ice accretion under extreme weather conditions. A numerical modeling approach was applied using FENSAP ICE to simulate turbine blade icing and to determine the aerodynamic performance degradation due to ice accretion. Particular attention is paid to the combined effects of the cloud characteristics, i.e. median volume diameter (MVD), liquid water content (LWC) and ambient air temperature, in a relatively wide range that covers in-cloud icing and precipitation icing as well. Depending on these parameters, aerodynamic performance degradation may not occur proportionally with the increase in ice mass, which is discussed in detail. The accuracy of the numerical model is based on the number of shots, which is also studied. A single-shot approach means simulation of the icing event in a single step on the bare surface occurring over a period, whereas multi-shot involves multiple icing simulations, redefining the surface and applying mesh displacement after each shot. Such simulation considers that each additional layer of ice accretes on different iced surfaces. Numerical validation showed that a five-shot approach provided a close estimation of experimental results and was assessed sufficient for the study considering computational time and accuracy. The mass of ice accretion augments increases when LWC increases from 0.1 g/m^3 to 1 g/m^3, and when MVD increases from 20 μm to 100 μm, which results in the decrease of the lift-to-drag ratio (CL/CD) after a long enough accretion time. Higher ice mass leads to aerodynamic performance degradation; however, a slight increase in the ratio CL/CD may be observed after short accretion time for up to 20 minutes.

Keywords: Aerodynamic performance, ice accretion, liquid water content (LWC), median volume diameter (MVD), wind turbine

1. Introduction

Wind power is becoming a prevalent global source of electricity to reduce climate change effects [1–3]. However, wind energy penetration is affected by atmospheric conditions, location, and polar vortex [4]. The polar vortex expands during winters, sending colder air from the Arctic to mid-latitudes that can cause winter storms in areas that are not typically associated with cold. The cold spells associated with icing conditions cause ice accumulation on wind turbine blades, reducing power production [5, 6]. The regions with high wind energy potential mainly lie in the cold climatic regions due to higher air densities that can increase power by about 10% [7, 8]. The icing regions pose a great danger to wind power production and energy transmission due to ice accumulation and ice load, which may lead to a shutdown or stall of wind turbines, affecting the grid stability [9]. The frequency of icing in a region greatly influences power production due to stall standby on turbines during icing days. Botta [10] presented a case of Acqua Spruzza Italy receiving 12 to 36 icing days per year. Maissan [11] studied the icing days of the Whitehorse region in Canada, with 33 to 50 icing days annually resulting in 20% estimated energy production loss. Dierer et al. [12] studied the icing frequency in the winter of 2009/2010 on an E-82 Enercon turbine in the Jura region of Switzerland, with results showing 11.5 and 41.5 days/year of meteorological icing and instrumental icing, respectively. The analyzed power reduction from the region with and without heating instruments on the blade showed a 3.5% and 10% annual power reduction, respectively. The impact of icing on wind energy involves wind power penalties because of structural vibrations of the overloaded component, which results in fatigue of wind turbine components, rotational imbalance, and an increase in drag force due to the formation of a new shape affecting the airflow [13, 14]. Paper [15] studied numerically the performace losses on an Aelos 30kW airfoil due to an icing event and obtained a result of 24% power loss from the 2D flow analysis; hence there is a need to study the power reduction due to icing.

Atmospheric icing conditions are responsible for ice accretion, which is characterized by physical and atmospheric parameters such as blade design (airfoil shape), temperature, air density, liquid water content (LWC), relative humidity, and median volume diameter (MVD) of droplets in the natural cloud that the wind turbine is exposed to [16–21]. The blade design is determined by size, rotational speed, impact angle on the root to tip of the airfoil, the droplet impingement area, and the angle of attack. Virk et al. [22] showed that blade size and the shape of the airfoil profile exposed to ice accretion influenced power loss due to aerodynamic performance degradation. Reid et al. [23] performed a study on the rotation of wind turbines under icing conditions, finding aerodynamic performance degradation leading to a 60% power reduction.

Icing conditions depend on the physical and atmospheric conditions, which are classified as in-cloud icing and precipitation icing. In-cloud icing is formed when the supercooled droplets collide with an object (e.g. a wind turbine blade), which changes the thermodynamic conditions, causing freezing. In-cloud icing results in rime ice or glaze ice, depending on the ambient parameters, principally the temperature, MVD, and LWC. Glaze ice is formed during wet ice growth associated with droplet diameter up to $500\,\mu m$ and high LWC, whereas rime ice is formed with temperatures below -6 C°, small MVD up to about 10, and lower LWC in the range of 0.1 g/m^3 [17, 22]. Paper [23] carried out a study on the performance degradation of a wind turbine using FENSAP-ICE with LWC of 0.5 g/m^3, MVD between $20 - 30\,\mu m$, temperature of $-3\ ^{\circ}C$ and $-15\ ^{\circ}C$ and accretion time between 10-60 minutes. They observed how icing was influenced by atmospheric conditions and showed the relationship between the LWC, MVD, and temperature that results in similar icing conditions. The LWC decreases with increase in temperature in some scenarios [24].

Despite the challenges associated with the impact of icing on power production and targeting the increasing use of renewable energy, it is crucial to evaluate wind turbine performance under extreme weather conditions to obtain useful data to improve wind turbine performance in icing regions. Data collection on wind turbine icing is challenging due to unpredictable factors such as number of icing days, uncontrolled changes in atmospheric conditions, and inaccurate images captured by cameras [25]. The icing scenarios are studied by numerical tests applying computational fluid dynamics (CFD) and by laboratory tests in icing wind tunnels to predict ice formation under controlled conditions [26].

This study applies a numerical approach to model icing on a wind turbine blade section using ANSYS FENSAP ICE 2021/R2. The software applies a single-shot or multi-shot approach, the latter one providing more accurate but more costly computation. Raj et al. [27] studied the impact of nunber of shots for single shot, 4 shots and 8 shots and concluded that using multi-shots was more effective compared to a single shot. However, they did not focus on determining the minimum number of shots that can be used with minimal impact on the accuracy of aerodynamic performance. Wang et al. [28] carried out a numerical study on a NACA 0012 airfoil with shots between a single shot to 5 shots under varying icing conditions, but mostly focused on the impact of ice shapes.

In the present study, the ice accretion is simulated, and the optimum number of shots in the numerical model is determined, which provides acceptable accuracy and helps reduce computational time. The ice mass and the corresponding aerodynamic performance are evaluated under a wide enough range of cloud characteristics that covers substantially different icing conditions. The study will reveal how the aerodynamic performance considered by the lift-to-drag ratio changes with accretion time. The results provide beneficial information for researchers in the wind industry and contribute to more efficient energy production under extreme weather conditions.

2. Numerical model

2.1. **Geometry and computational domain.** The study employed a C-shaped computational domain around a NACA4412 airfoil. This shape was considered due to its moderate thickness, which can be used in several applications including aviation and wind turbines and thus providing versatility for numerical simulations under different conditions. The NACA 4412 airfoil with a 1 m chord length was defined and extruded 1 m in spanwise direction since FENSAP-ICE works with a 3D geometry, but the unsteady flow was simulated in the plane determined by the airfoil section. A fine 2D grid was created with 98,573 elements, a minimum orthogonal quality, and a maximum skew of 0.85 and 0.194 respectively. Triangular meshing in the domain was used in the study with a higher resolution near the blade surface for better accuracy, characterized by 1.05% growth of cells outwards, with dense elements and nodes occurring close to the wall. To accurately capture the flow phenomenon, the wall/airfoil was divided into small domains (1000 units) all around and the inflation mesh of 27 layers was introduced with first layer thickness derived in ANSYS FENSAP-ICE (2017):

$$y^+ = \frac{y u_\tau}{v} = \frac{y}{\delta}, \tag{1}$$

where y is the distance from the wall to a point of interest, δ is the molecular viscous length scale, v is the kinematic viscosity, and u_τ is the friction velocity.

The no-slip condition was achieved through the distance separation displayed on the number of layers and the boundary layer characteristic on the transition and separation which guided in the laminar-turbulent transition. The first layer thickness calculated was 1.46 m with a growth rate of 1.08% outwards to fully capture the complex ice shape and mass from the flow distribution over the surface and last inflation layer had a thickness of 1.9406×10^{-5} m. The number of layers was within the range specified in a study done by Piperas [29] (i.e. < 100 layers) for reducing the computational cost, especially in complex simulations, while maintaining the mesh quality.

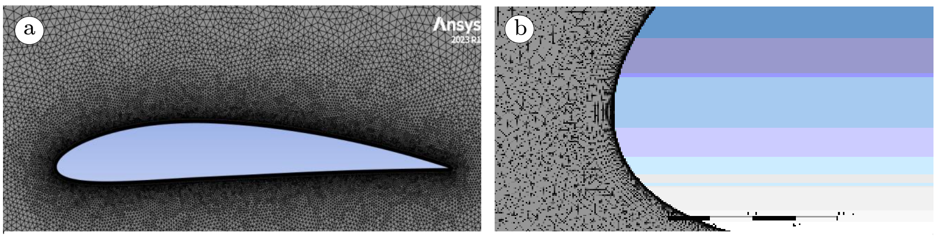

Figure 1. Mesh around the blade: (a) Fine, unstructured mesh (triangular mesh); (b) meshed domain near the leading edge

2.2. **Boundary and flow conditions.** The boundary conditions play an important role in the accuracy and reliability of the simulation by describing the inlet, outlet, wall, and symmetry conditions. The boundary conditions used in the study employed the Dirichlet and Neumann conditions in specifying the value of the solution and the derivative of the solution, respectively. The inlet condition is specified as the velocity with 20 m/s used in the study, the outlet condition specifies the pressure or the backflow condition in the outlet, and the gage pressure was set to 0 Pa. The ambient temperature in the freestream was defined as $-5\ ^\circ C$, $-10\ ^\circ C$ and $-20\ ^\circ C$. The airfoil in the study was set to be an obstacle with wall temperature initialized by isothermal conditions at $+0.1\ ^\circ C$ higher than freestream ambient temperature, while the symmetry conditions are used to describe the boundaries within which the flow occurs. These boundary conditions are indicated in Figure 2. Based on studies done by Abdalkarem et al. [30] and Manni et al. [31], it was found that utilizing the computational domain having a distance of 10 to 15 times chord length downstream was ideal for the study. The distance upstream from the leading edge was set at 5-chord lengths, while downstream from the trailing edge to the end of domain at 10-chord lengths.

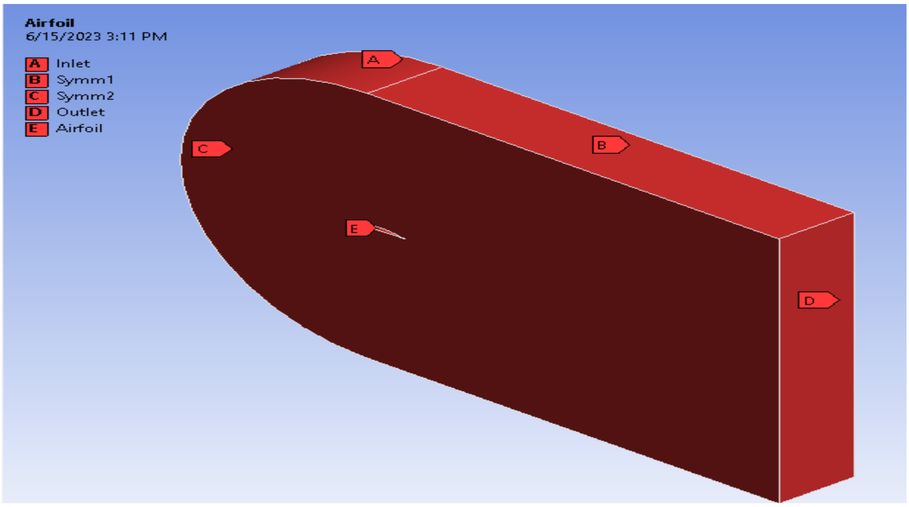

Figure 2. C-shaped computational domain

2.3. **Icing model.** Icing is a complex phenomenon involving phase change and thermodynamic and fluid dynamic processes when the supercooled droplets hit the surface and accrete. The rate of icing is calculated using FENSAP-ICE, as summarized in the following steps. First, the flow around the airfoil is determined by the flow solver (FENSAP), then the motion of droplets is simulated by the droplet's solver (DROP3D), and finally icing is modeled by the ice accretion and water runback module (ICE3D).

The cloud that leads to ice accretion is modeled by multiphase flow over the airfoil surface governed by Reynolds-Averaged Navier-Stokes (RANS) equations coupled with Lagrangian particle tracking. The continuity equation ensures that the mass of the fluid is conserved within the simulation domain, while the momentum equation describes the conservation of momentum within the fluid. The k-turbulence model was used in the present study, which derived the dynamic eddy viscosity and the bulk fluid viscosity over the fluid flow. This model was developed by Menter to blend the robust and accurate nature of $k \cdots \omega$ model in near-wall region varying with models, i.e., $k \cdots \varepsilon$ and $k \cdots \omega$ [32, 33]. The blending function on the $k \cdots \omega$ SST model is used for smooth transition between the models based on the distance from the wall. The $k \cdots \varepsilon$ is suitable for capturing turbulent regions in far distances, while $k \cdots \omega$ is activated near the wall where boundary layer turbulence is significant, and is thus able to resolve flow dynamics.

Water droplet trajectories near the surface are modeled by the droplet equation, which describes the motion of individual droplets in a fluid based on the assumptions that droplets do not collide, coalesce, or splash until they reach the surface. Numerically, the ice accretion involves a multiphase-flow approach involving the tracking of trajectories of supercooled water droplets, which determines the collection efficiency on the surface, followed by the heat transfer governing the air-liquid-solid phase change and ice accretion on the airfoil. The ice characteristics based on the physical and atmospheric conditions determines the type of ice as described in Ibrahim et al. [17] and Rotich & Kollár [19]. Factors which mainly affect the accretion process include the atmospheric conditions (microphysics) described by the ambient temperature Ta, liquid water content (LWC), and median volume diameter (MVD), whereas physical components include airfoil configuration (angle of attack).

The thermodynamics of the ice accretion process as described in Makkonen et al. [34] determine the accretion efficiency that affects the rate of icing. Icing over the surface was numerically simulated after defining the atmospheric conditions influencing the aerodynamic performance and ice shapes. The controlled conditions set were air temperature (-5, -10, and -20 $-20\,°C$), LWC (0.1 g/m^3, 0.5 g/m^3, and 1 g/m^3), MVD (20, 40, 60, 80 and 100 µm) at 0° angle of attack and accretion time of 3 hours. The numerical parameter, the number of shots in the simulation of the icing, was varied from a single shot to multi-shot including 3-5-8 shots, which has an impact on the ice shape and mass and the aerodynamic performance degradation. A single-shot simulation involves constant one-interval ice accretion over a given time, while a multi-shot approach is divided into shorter-interval icing solutions obtained after dividing the total icing time by the number of shots (3600, 2160 and 1350 seconds for 3, 5 and 8 shots, respectively, in this study). Grid on the airfoil surface is defined in the first shot, and then it is displaced in each shot according to the iced airfoil profile, with more shots causing formation of a more complex shape. Atmospheric conditions are set in each shot, then the droplet impingement is simulated on the iced surface, further ice accretion is predicted, and the aerodynamic performance of the iced blade is determined.

3. Results and discussion

The airfoil section studied was NACA4412. The FENSAP solver computed flow field solutions, while the droplet trajectories were calculated in DROP3D after setting up the conditions determined by the MVD, LWC, and droplet size distribution (Langmuir D) of the cloud. Icing prediction was based on numerical calculations in the ICE3D. The numerical model will be validated first in this section, followed by analyzing the impact of number of shots on icing and on aerodynamic performance. Finally, the effects of MVD, LWC, and air temperature will be discussed.

3.1. **Validation of the numerical model.** The grid independence study was carried out to determine the number of divisions and elements in the mesh generated. The classification of the refinement was done based on the number of divisions in the domain.

According to a study conducted by Roache [35], the accuracy of numerical solutions may be assessed using the discretization method. The estimation on the accuracy

Table 1. Grid refinement ratio obtained depending on the number of elements

Divisions	35	100	400	800	1200	1500	2000
Elements	84525	87845	181215	354330	497515	651970	900990
Refinement ratio		1.039278	2.062895	1.955302	1.404101	1.310453	1.38195

of solution was based on calculating the grid refinement ratios. According to Roache, using Richardson extrapolation theory (Celik et al. [36]) a refinement ratio greater than 1.3 was ideal for numerical studies. In the present scenario, medium/coarse was not found to be ideal since the refinement ratio was 1.039; however, it increased to 2.063 for fine/medium, which was found to be excellent.

The lift-to-drag ratio is plotted as a function of the number of elements in Figure 3 to show that the aerodynamic performance is not affected by further increasing the number of divisions above the chosen value.

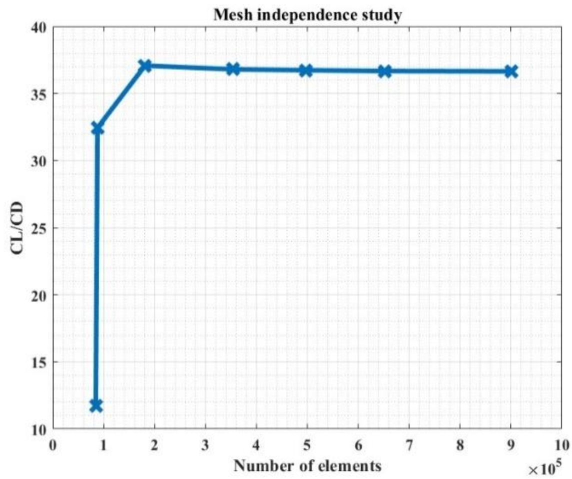

Figure 3. Results of grid independence study regarding lift-to-drag ratio

The numerical model was validated by an experimental study carried out in a low-speed wind tunnel by Sundaresan et al. [37] using the NACA0012 airfoil. The conditions used in the experimental study were wind speed of 77 m/s, MVD of $20\,\mu m$, LWC of $0.5\,\mathrm{g/m^3}$ and 16.9 minutes accretion time for an airfoil with 0.533 m chord length, which was duplicated and numerically simulated on FENSAP-ICE software. In the numerical study, single shot and 3-5-8 shot simulations were applied. Figure 4 shows that similar ice shapes were obtained after the 5-shot and 8-shot simulations. The single-shot and 3-shot simulations slightly underestimate the amount of ice on the upper half of the profile, and they predict the maximum ice thickness at a lower position. However, the simulations with five and eight shots

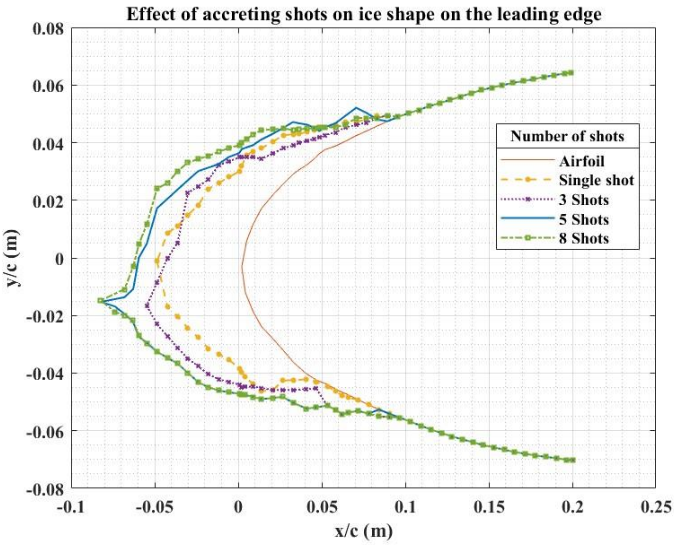

Figure 4. Comparison of ice accretions on NACA 4412 profile obtained numerically for single-shot and multi-shot simulations

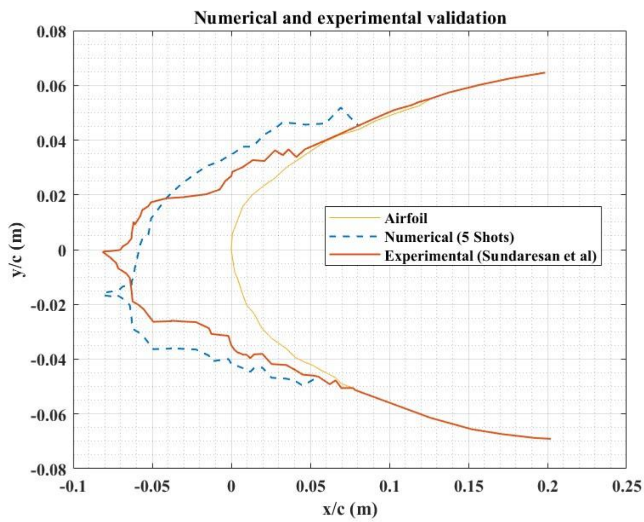

Figure 5. Comparison of numerical results (5 shots) obtained by FENSAP-ICE 2021 R2 with experimental data from low-speed subsonic wind tunnel facility (Sundaresan et al. [37]) from airfoil generated by Jacobs et al. [38].

provide a nearly similar shape of ice formed on the leading edge to that obtained experimentally, as can be compared in Figure 5.

3.2. **Impact of number of shots on the accuracy of model prediction.** The atmospheric and physical conditions listed in Section 2.2 were assumed in the numerical study and were introduced in FENSAP-ICE. The assumptions made in the study were that droplets were spherical and no coalescence, splashing/bouncing, or fragmentation or disruption occurred in the simulation of a three-hour ice accretion event. In the following, the changes in the ice mass and in the lift-to-drag ratio when increasing the number of shots are compared.

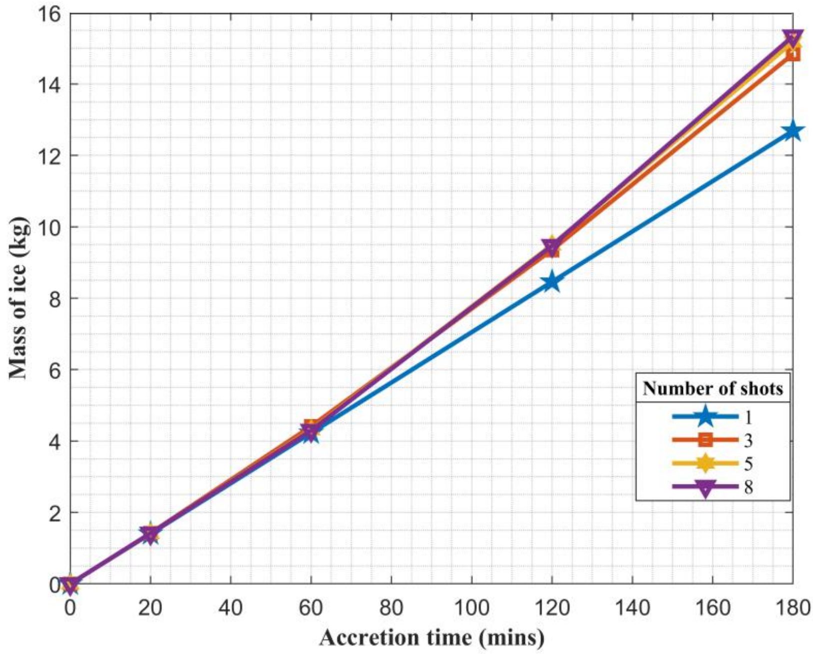

Figure 6. Effect of number of shots on the mass of ice for different accretion times (mins), for LWC $1\,\mathrm{g/m^3}$, MVD $100\,\mu m$ and air temperature $-10\,^{\circ}C$

According to Figure 5, the ice mass did not vary significantly with the number of shots, except between the single-shot and multi-shot simulations after long accretion time. The differences after 180 imin accretion time for an MVD of $100\,\mu m$ were 14.88% between 1 and 3 shots, 2.24% between 3 and 5 shots, and 1.04% between 5 and 8 shots. The ice accretion depended on the number of shots and affected the flow over the surface, forming a more streamlined shape on the leading edge for the single shot. The mass of ice increases with the number of shots, and once the prediction of ice shape becomes accurate enough, the ice mass does not change considerably with the number of shots. The aerodynamic performance degradation may be evaluated by the reduction in the lift-to-drag ratio CL/CD. Figure 7 reveals how this parameter varied with the number of shots for different values of LWC. The variation in the lift-to-drag ratio with the number of shots is below 5% for the smallest LWC, as seen for $0.1\,\mathrm{g/m^3}$. However, it is 20-50% for higher LWC when increasing the number of shots up to 5, and then further increasing the number of shots from 5 to 8, the change reduces to around or below 5%.

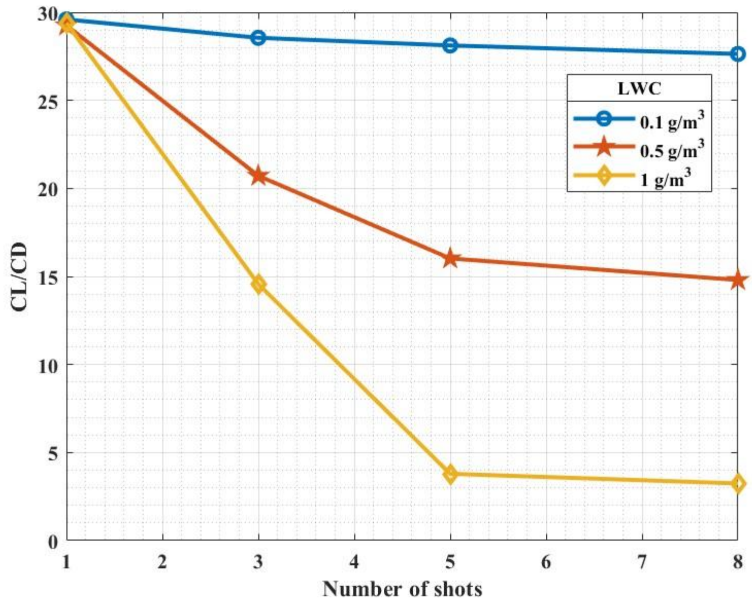

Figure 7. Effect of the number of shots on aerodynamic performance for MVD 60 μm, accretion time 180 minuts, air temperature $-10\,°C$, and for different values of LWC $\mathrm{g/m^3}$

The lift-to-drag ratio reduces significantly when the number of shots increases up to five. However, no significant difference can be observed between the lift-to-drag ratios obtained with the five- and the eight-shot simulations. Consequently, increasing the number of shots above five does not lead to further considerable change in ice shape or in aerodynamic performance degradation. Furthermore, a high number of shots leads to numerical instability, as was observed in some simulations that were run with 20 shots [39]. Therefore, this study employs five shots in the following in order not to overly increase the computation time and to avoid numerical problems.

3.3. **Effects of MVD and LWC.** The icing rate and mass of ice accreting on the airfoil depend on atmospheric conditions described by parameters such as LWC and MVD. When LWC and MVD are small, fewer droplets freeze, causing a slower accretion process on the surface, whereas large-diameter droplets collide more efficiently, and then they freeze, leading to an increase in ice mass. The inertial forces have little effect on small droplets that follow the streamlines, while greater droplets have higher inertia, causing increasing collision efficiency and impingement of a higher number of droplets. The collision efficiency is influenced by the droplet diameter, and the accretion efficiency depends on the availability of water on the surface that creates the nucleation sites for ice growth.

The ice mass was found to increase approximately linearly with the LWC, MVD, and accretion time (see Figure 8). These observations correspond to those reported in the studies by Hakimian et al. [40], Molkoselka et al. [41], and Tsao & Anderson, [42].

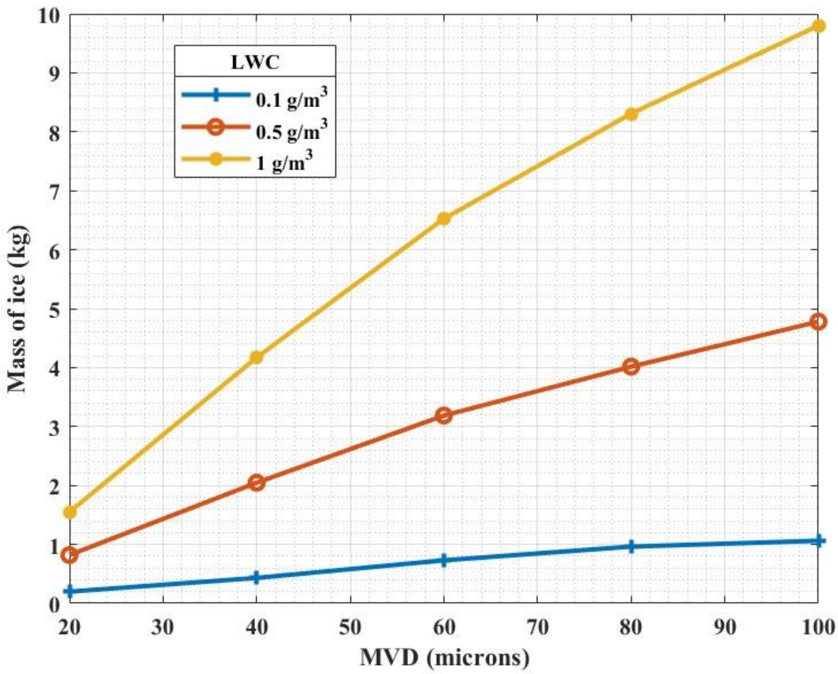

Figure 8. Effect of the number of shots on aerodynamic performance for MVD 60 μm, accretion time 180 minutes, air temperature $-10\,°C$, and for different values of LWC $\mathrm{g/m^3}$

Figure 8 represents how the accreted ice mass is affected by MVD and LWC. As MVD and LWC increase, the collection efficiency on the airfoil surface increases leading to more ice accreting on the leading edge. The horn formation that can be seen in Figure 9 is substantially influenced by the droplet diameter. The ice accreted on the surface for lower MVD causes little or no noticeable flow separation compared to the ice accretion obtained for higher MVD, which forms a complex shape creating recirculation flow. The iced airfoil shape alters the flow over the surface, increasing the drag and resulting in a separation region further along the upper profile behind the leading edge.

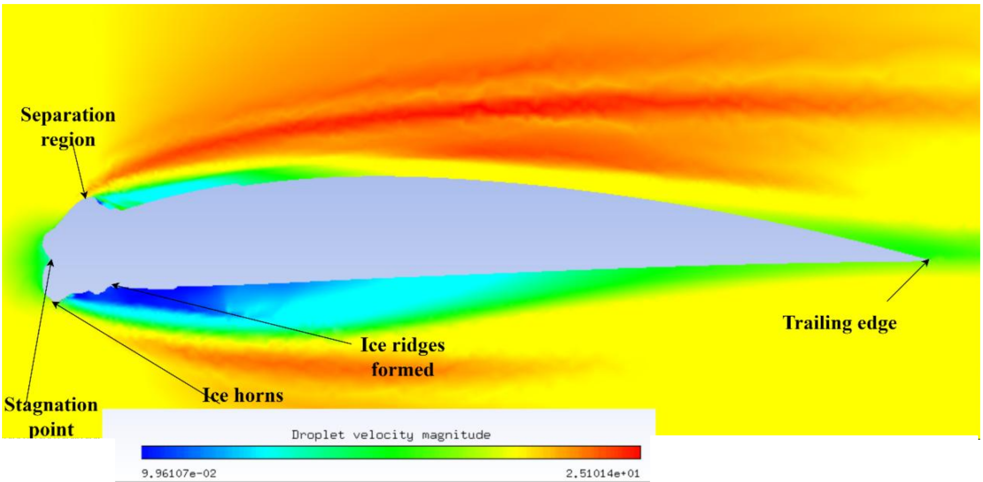

Figure 9. Flow distribution disturbance caused by ridges of ice accretion, for LWC 0.5 g/m^3, MVD 100 μm, air temperature $-20\,°C$, accretion time 180 minutes

Ice accretion causes aerodynamic degradation, since the lift decreases and the drag increases. However, an unexpected tendency was observed after a short accretion time. A small amount of ice on the blade may even slightly increase the lift-to-drag ratio, which is followed by a steep decrease after further ice accretion due to shift of the stagnation point (Rotich & Kollár [19]) and the flow separation described in the previous paragraph. These tendencies can be observed in Figure 10, where

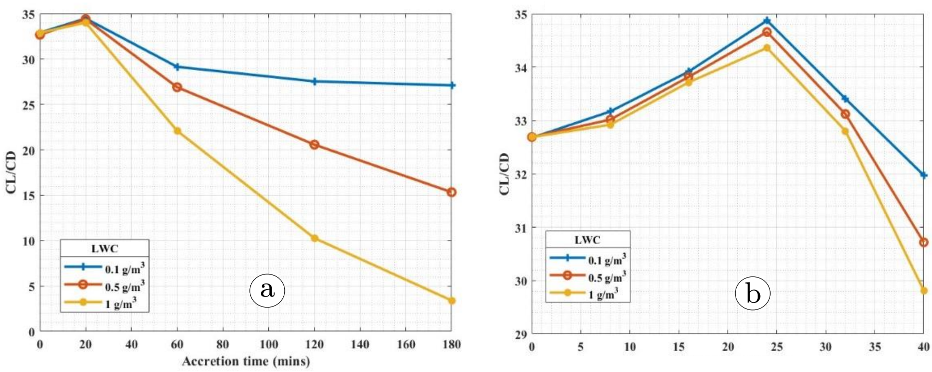

Figure 10. Variation of lift-to-drag ratio with accretion time (mins) for different values of LWC, at MVD 60 μm and air temperature $-10\,°C$: (a) accretion time is 180 min; (b) short accretion times up to 40 minutes

results of simulations with smaller time intervals are shown in Figure 10(b). The aerodynamic degradation in 180-minute accretion time is greatly affected by the LWC. The reduction in the lift-to-drag ratio is less than 20% for the smallest LWC, while it drops to about one tenth for the highest LWC. The ice type on the surface is mainly determined by the LWC and MVD. Rime ice is formed when droplets are small and LWC is low, whereas higher LWC and MVD increase the chance of forming glaze ice due to the higher water content available on the surface, leading to incomplete freezing. The ice shape is also greatly affected by MVD and LWC. Bigger droplets result in greater collision efficiency, leading to increased ice accretion with with the appearance of horns and less streamlined airfoils (Virk et al. [43]). An increase in LWC results in a higher amount of liquid water on the surface, which influences the type of accreting ice and worsens the aerodynamic characteristics.

3.4. **Effects of air temperature.** The atmospheric temperature influences the rate of icing and the type of ice on the airfoil surface. At higher temperatures, the heat transfer is not enough to freeze all droplets upon impact, causing some runback water on the airfoil surface leading to glaze ice. At lower temperatures, the supercooled water droplets freeze immediately upon impact, causing rime ice. The effect of temperature on ice shape and aerodynamic performance was studied on $-5\,°C$, $-10\,°C$, and $-20\,°C$ (Figure 11). In FENSAP-ICE, the icing solver considers the heat balance

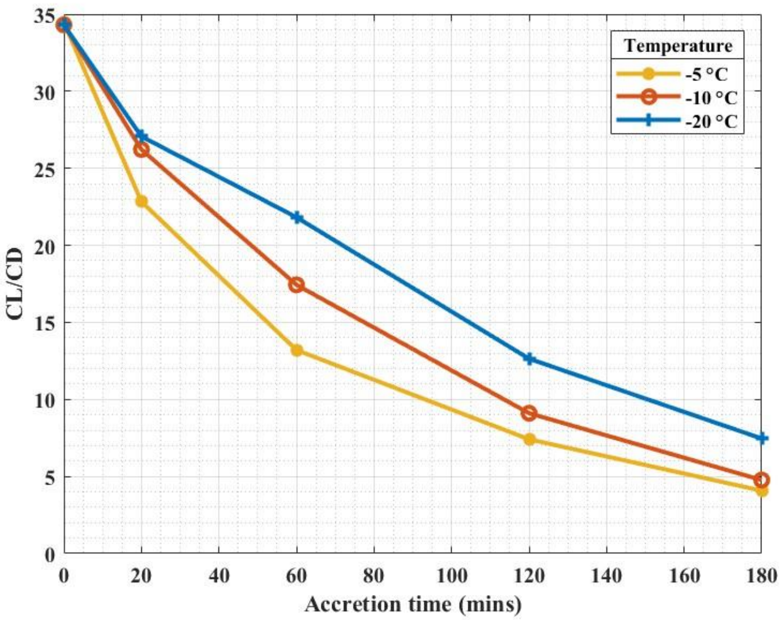

Figure 11. Effect of air temperature on lift-to-drag ratio for MVD $80\,\mu m$ and for LWC $1\,\mathrm{g/m^3}$

between the liquid water and the accreted surface. Figure 11 shows how the lift-to-drag ratio reduces with accretion time for different values of air temperature. Since the LWC is high (i.e. $1\,\mathrm{g/m^3}$), the lift-to-drag ratio decreases considerably with accretion time, but this decreasing tendency is faster at higher temperatures. Contrary to the results presented in Figure 9, the increasing tendency of the lift-to-drag ratio after the first 20 min accretion time cannot be observed in Figure 11. This may be explained by the higher MVD and high LWC. The ice in this case change the shape of the profile so that aerodynamic performance degradation occurs after even a few minutes of accretion.

The air temperature affects the ice formation and the water film on the surface (Orchard et al. [44]); thus, different shapes are formed at the leading edge for different air temperatures. At lower temperatures, the shape of the ice is more streamlined, while at higher temperatures, the ice has a 'horny' shape, as can be observed in Figure 12, and such changes in the shape influence the flow, and thus the aerodynamic performance.

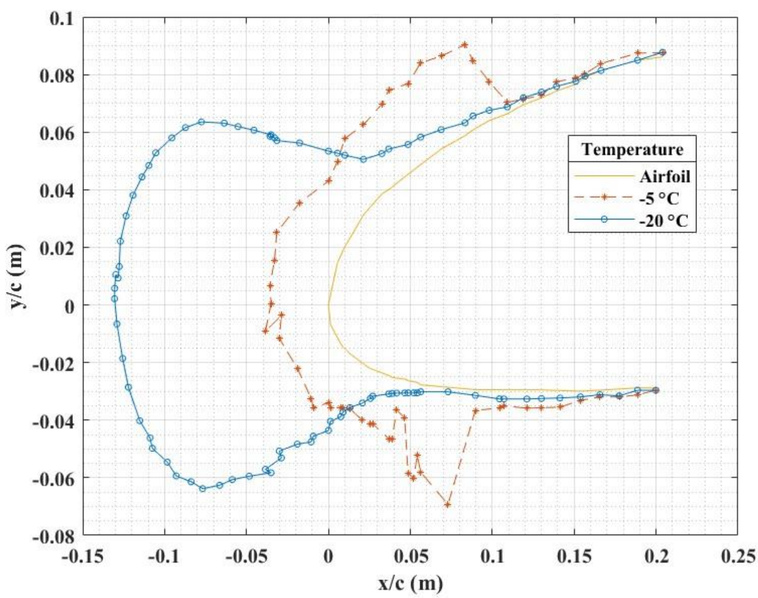

Figure 12. Effect of temperature on ice shape for MVD 80 μm, LWC $1\,\mathrm{g/m^3}$, at 180 minutes for $-5\,°C$ and $-20\,°C$

4. Conclusions

Ice accretion on the NACA4412 airfoil and the resulting aerodynamic performance degradation were modeled numerically. The optimum number of shots in the numerical simulation was determined and the effects of physical parameters describing the ambient conditions and the characteristics of the cloud were studied, including MVD, LWC, air temperature, and accretion time. The numerical approach was validated with experimental results, and the 5-shot and 8-shot approaches provided close prediction of ice shape and lift-to-drag ratio contrary to the single-shot and 3-shot simulations. The single-shot approach was found to be inaccurate for estimating ice mass after a long accretion time.

- i The lift-to-drag ratio changed considerably when the number of shots increased up to 5; however, further increasing it to 8 resulted in a change of 5% or less. Consequently, the 5-shot approach was chosen for further simulations.
- ii The MVD was varied from 20 mm to 100 mm, at 10 μm intervals, whereas the LWC was changed from 0.1 $g/m^3$to 1 g/m^3. Simulation results showed that ice mass increased with both parameters. Aerodynamic performance degradation was concluded to be more significant for higher values of MVD and LWC.
- iii An interesting property was also observed depending on the ambient parameters. The lift-to-drag ratio that was used to describe aerodynamic performance slightly increased after a short period of ice accretion (i.e., up to 20-25 minutes), and dropped only after further ice accretion. Thus, a small amount of ice may not cause aerodynamic performance degradation at smaller values of MVD and LWC.
- iv The air temperature influences ice formation, since horny shapes develop for higher temperature, i.e., when the temperature is closer to the freezing point. Consequently, the lift-to-drag ratio reduces to lower values for higher air temperatures.

Further research will include experimental study of the effects of the ambient parameters on ice accretion in an icing wind tunnel and the consideration of these results in the design of blade shapes. Such observations would contribute to extending the operation of wind turbines under icing conditions.

Acknowledgement. Project no. TKP2021-NVA-29 has been implemented with support provided by the Ministry of Culture and Innovation of Hungary from the National Research, Development, and Innovation Fund, financed under the TKP2021-NVA funding scheme.

References

1. Jung, C. and Schindler, D. "Development of onshore wind turbine fleet counteracts climate change-induced reduction in global capacity factor." *Nature Energy,* **7**, (2022), 608–619. doi: 10.1038/s41560-022-01056-z.
2. Rotich, I. K. and Musyimi, P. K. "Wind power density characterization in arid and semi-arid Taita-Taveta and Garissa counties of Kenya." *Cleaner Engineering and Technology,* (2023), p. 100704. doi: 10.1016/j.clet.2023.100704.
3. Suman, A. "Role of renewable energy technologies in climate change adaptation and mitigation: A brief review from Nepal." *Renewable and Sustainable Energy Reviews,* **151**, (2021), p. 111524. doi: 10.1016/j.rser.2021.111524.

4. Salam, A., Alsabagh, Y., Xu, Y., Virk, M. S., Suman, A. and Badran, O. "Atmospheric ice loading and its impact on natural frequencies of wind turbines. Wind Engineering." *Wind Engineering,* **39**(1), (2015), 83–96. DOI: 10.2307/90006861.
5. Zhang, J., Yue, P., Zhang, Q. and Wang, Z. "Impact of tropospheric polar vortex on winter cold extremes over Northeast China." *Atmospheric Research,* **294**, (2023), p. 106942. DOI: 10.1016/j.atmosres.2023.106942.
6. Chuang, Z., Yi, H., Chang, X., Liu, H., Zhang, H. and Xia, L. "Comprehensive analysis of the impact of the icing of Wind turbine blades on power loss in cold regions." *Journal of Marine Science and Engineering,* **11**(6), (2023), p. 1125. DOI: 10.3390/jmse11061125.
7. Fortin, G., Perron, J. and Ilinca, A. *Behaviour and modeling of cup anemometers under icing conditions.* IWAIS XI. URL: https://www.researchgate.net/publication/259758149.
8. Fu, P. and Farzaneh, M. "A CFD approach for modeling the rime-ice accretion process on a horizontal-axis wind turbine." *Journal of Wind Engineering and Industrial Aerodynamics,* **98**(4-5), (2010), 181–188. DOI: 10.1016/j.jweia.2009.10.014.
9. Gao, L. and Hong, J. "Wind turbine performance in natural icing environments: A field characterization." *Cold Regions Science and Technology,* **181**, (2011), p. 103193. DOI: j.coldregions.2020.103193.
10. Botta, G., Cavaliere, M. and Holttinen, H. *Ice accretion at Acqua Spruzza and its effects on wind turbine operation and loss of energy production.* BOREAS IV. URL: https://www.researchgate.net/publication/265244514.
11. Maissan, J. F. "Wind power development in sub-arctic conditions with severe rime icing." *Circumpolar Climate Change Summit and Exposition,* (2011), 174–183. URL: https://thenorthernreview.ca/index.php/nr/article/view/233/226.
12. Dierer, S., Oechslin, R. and Cattin, R. "Wind turbines in icing conditions: performance and prediction." *Advances in Science and Research,* **6**(1), (2011), 245–250. DOI: 10.5194/asr-6-245-2011.
13. Kollar, L. E. and Mishra, R. "Inverse design of wind turbine blade sections for operation under icing conditions." *Energy Conversion and Management,* **180**, (2019), 844–858. DOI: 10.1016/j.enconman.2018.11.015.
14. Manatbayev, R., Baizhuma, Z., Bolegenova, S. and Georgiev, A. "Numerical simulations on static vertical axis wind turbine blade icing." *Renewable Energy,* **170**, (2021), 997–1007. DOI: 10.1016/j.renene.2021.02.023.
15. Yirtici, O., Tuncer, I. H. and Ozgen, S. "Ice accretion prediction on wind turbines and consequent power losses." *Journal of Physics: Conference Series,* **753**, (2016). DOI: 10.1088/1742-6596/753/2/022022.
16. Dhyani, A., Choi, W., Golovin, K. and Tuteja, A. "Surface design strategies for mitigating ice and snow accretion." *Matter,* **5**(5), (2021), 1423–1454. DOI: 10.1016/j.matt.2022.04.012.
17. Ibrahim, G. M., Pope, K. and Muzychka, Y. S. "Effects of blade design on ice accretion for horizontal axis wind turbines." *Journal of Wind Engineering*

and Industrial Aerodynamics, **173**, (2018), 39–52. DOI: 10.1016/j.jweia.2017.11.024.

18. Kraj, A. G. and Bibeau, E. L. "Phases of icing on wind turbine blades characterized by ice accumulation." *Renewable Energy,* **35**(5), (2010), 966–972. DOI: 10.1016/j.renene.2009.09.013.
19. Rotich, I. and Kollár, L. E. "Numerical simulation of the performance of an asymmetrical airfoil under extreme weather conditions." *Mérnöki És Informatikai Megoldások,* **3**(2), (2022), 19–29. DOI: 10.37775/EIS.2022.2.2.
20. Strauss, L., Serafin, S. and Dorninger, M. "Probability forecasts of ice accretion on wind turbines derived from multiphysics and neighbourhood ensembles." *Quarterly Journal of the Royal Meteorological Society,* **148**(746), (2022), 2446–2467. DOI: 10.1002/qj.4311.
21. Swenson, L., Gao, L., Hong, J. and Shen, L. "An efficacious model for predicting icing-induced energy loss for wind turbines." *Applied Energy,* **305**, (2022), p. 117809. DOI: 10.1016/j.apenergy.2021.117809.
22. Virk, M., Homola, M. and Nicklasson, P. "Atmospheric icing on large wind turbine blades." *International Journal of Energy and Environment,* **3**(2), (2012), pp. 1–8.
23. Reid, T., Baruzzi, G., Ozcer, I., Switchenko, D. and Habashi, W. *FENSAP-ICE simulation of icing on wind turbine blades, Part 1: performance degradation.* 51st AIAA Aerospace Sciences Meeting Including the New Horizons Forum and Aerospace Exposition, Jan. 7. DOI: 10.2514/6.2013-750.
24. Liu, Y., Zhang, K., Tian, W. and Hu, H. "An experimental investigation on the dynamic ice accretion and unsteady heat transfer over an airfoil surface with embedded initial ice roughness." *International Journal of Heat and Mass Transfer,* **146**, (2020), p. 118900. DOI: 10.1016/j.ijheatmasstransfer.2019.118900.
25. Han, Y., Palacios, J. and Schmitz, S. "Scaled ice accretion experiments on a rotating wind turbine blade." *Journal of Wind Engineering and Industrial Aerodynamics,* **109**, (2012), 55–67. DOI: 10.1016/j.jweia.2012.06.001.
26. Homola, M. C., Virk, M. S., Wallenius, T., Nicklasson, P. J. and Sundsbø, P. A. "Effect of atmospheric temperature and droplet size variation on ice accretion of wind turbine blades." *Journal of Wind Engineering and Industrial Aerodynamics,* **98**(12), (2010), 724–729. DOI: 10.1016/j.jweia.2010.06.007.
27. Raj, L., Yee, K. and Myong, R. S. "Sensitivity of ice accretion and aerodynamic performance degradation to critical physical and modeling parameters affecting airfoil icing." *Aerospace Science and Technology,* **98**, (2020), p. 105659. DOI: 10.1016/j.ast.2019.105659.
28. Wang, Q., Yi, X., Liu, Y., Ren, J., Li, W., Wang, Q. and Lai, Q. "Simulation and analysis of wind turbine ice accretion under yaw condition via an improved multi-shot icing computational model." *Renewable Energy,* **162**, (2020), 1854–1873. DOI: 10.1016/j.renene.2020.09.107.

29. Piperas, A. T. "Investigation of boundary layer suction on a wind turbine airfoil using CFD (MSc thesis)." PhD thesis. Technical University of Denmark, 2010.
30. Abdalkarem, A. A. M., Abdullah, A. F., Sopian, K., Haw, L. C., Muzammil, W. K. and Wong, K. H. "The effect of trailing-edge wedge-tails on the aerodynamic characteristics of wind turbine airfoil." *IOP Conference Series: Materials Science and Engineering,* **1278**(1), (2023), p. 012011. doi: 10.1088/1757-899X/1278/1/012011.
31. Manni, L., Nishino, T. and Delafin, P. L. "Numerical study of airfoil stall cells using a very wide computational domain." *Computers & Fluids,* **140**, (2016), pp. 260–269. doi: 10.1016/j.compfluid.2016.09.023.
32. Martini, F., Ibrahim, H., Contreras Montoya, L. T., Rizk, P. and Ilinca, A. "Turbulence modeling of iced wind turbine airfoils." *Energies,* **15**(22), (2016), p. 8325. doi: 10.3390/en15228325.
33. Menter, F. *Zonal two equation $k-\omega$ turbulence models for aerodynamic flows.* 23rd Fluid Dynamics, Plasmadynamics, and Lasers Conference, July 6. doi: 10.2514/6.1993-2906.
34. Makkonen, L., Laakso, T., Marjaniemi, M. and Ilinca, A. "Modelling and prevention of ice accretion on wind turbines." *Wind Engineering,* **25**(1), (2001), pp. 3–21. doi: 10.1260/0309524011495791.
35. Roache, P. J. "Perspective: A method for uniform reporting of grid refinement studies." *Journal of Fluids Engineering,* **116**(3), (1994), pp. 405–413. doi: 10.1115/1.2910291.
36. Celik Ismail B., Ghia Urmila, Roache Patrick J., Freitas Christopher J., Coleman Hugh and Peter E. Raad. "Procedure for estimation and reporting of uncertainty due to discretization in CFD applications." *Journal of Fluids Engineering,* **130**(7), (2008), p. 078001. doi: 10.1115/1.2960953.
37. Sundaresan, A., Arunvinthan, S., Pasha, A. A. and Pillai, S. N. "Effect of ice accretion on the aerodynamic characteristics of wind turbine blades." *Wind and Structures, An International Journal,* **32**(8), (2021), 205–217. doi: 10.12989/was.2021.32.3.205.
38. Jacobs, E. N., Ward, K. E. and Pinkerton, R. M. *The characteristics of 78 related airfoil sections from tests in the variable-density wind tunnel.* in NASA. 1935.
39. Rotich, I. and Kollár, L. "Numerical simulation of the performance of an asymmetrical airfoil under extreme weather conditions." *Mérnöki és Informatikai Megoldások,* **3**(2), (2013), pp. 19–29. doi: 10.37775/EIS.2022.2.2.
40. Hakimian, A., Nazifi, S. and Ghasemi, H. *Ice Adhesion: Mechanism, Measurement and Mitigation.* Ed. by K. L. Mittal and C. H. Choi. Wiley, 2020. Chap. Physics of Ice Nucleation and Growth on a Surface, 87–110. doi: 10.1002/9781119640523.ch3.
41. Molkoselka, E., Kaikkonen, V. and Makynen, A. *Instrument and method for measuring ice accretion in mixed-phase cloud conditions.* IEEE International Instrumentation and Measurement Technology Conference (I2MTC). 1-5., 2020. url: 10.1109/I2MTC43012.2020.9129604.

42. TSAO, J. C. and ANDERSON, D. N. *Additional study of water droplet median volume diameter (MVD) effects on ice shapes.* NASA, 2005. URL: http://www.sti.nasa.gov.
43. VIRK, M. S., HOMOLA, M. C. and NICKLASSON, P. J. "Effect of rime ice accretion on aerodynamic characteristics of wind turbine blade profiles." *Wind Engineering,* **34**(2), (2010), 207–218. DOI: 10.1260/0309-524X.34.2.207.
44. ORCHARD, D. M., CLARK, C. and CHEVRETTE, G. "Measurement of liquid water content for supercooled large drop conditions in the NRC's altitude icing wind tunnel." *The Japan Society for Aeronautical and Space Sciences* **54**(6), (2013), 175–186. DOI: 10.4271/2019-01-2007.